Extending the size-parameter range for plane-wave light scattering from infinite homogeneous circular cylinders

S. Hau-Riege

April 12, 2005

Disclaimer

Extending the size-parameter range for plane-wave light scattering from infinite homogeneous circular cylinders

Stefan P. Hau-Riege

Lawrence Livermore National Laboratory, P.O. Box 808, Livermore, CA 94551

Abtract

We have developed an algorithm that extends the possible size-parameter range for the calculation of plane-wave light scattering from infinite homogeneous circular cylinders using a Mie-type analysis. Our algorithm is based on the calculation of the ratios of Bessel functions instead of calculating the Bessel functions or their logarithmic derivatives directly. We have found that this algorithm agrees with existing methods (when those methods converge). We have also found that our algorithm converges in cases of very large size parameters, in which case other algorithms often do not.

1. Introduction

X-ray diffraction tomography has proven to be a powerful technique to determine the complex refractive-index distribution of weakly scattering objects [1-3]. Common test objects for diffraction tomography are cylindrically-shaped particles or cylindrical wires

[4] with diameters that are several orders of magnitude larger than the wavelength of the incident light. For verification purposes, it is often desirable to directly compare the measured scattering function or the scattering function calculated with other approximate methods to an exact analytical solution. Due to numerical instabilities, in the past these calculations have turned out to be challenging or impossible for large diameter-to-wavelength ratios. In this paper we present a new numerically-stable algorithm that enables one to perform these calculations on large cylinders.

An exact solution to the problem of scattering of electromagnectic plane waves from infinite homogeneous circular cylinders can be obtained using a Mie-type analysis. This has been described by numerous authors, see for example References [5-9]. The numerical evaluation of the involved equations is challenging, especially when cylinders are considered that have diameters that are much larger than the wavelength of the incident light. Some methods to perform these calculations in a numerically stable way have been suggested, for example by Bohren and Huffman [5] and Barber and Hill [6]. The problem of light scattering from spheres instead of cylinders has received much more attention [10-14], and quite sophisticated methods have been developed that allow the precise calculation of the scattered field even for large spheres with refractive indices with a large real or imaginary part. We have analyzed the methods suggested for spheres, and applied and extended them to circular cylinders. We have developed a numerically robust method for the calculation of scattering from cylinders even when the cylinder is large or has a large refractive index, i.e. for a parameter space in which other algorithms have failed.

In the following we will review how the Mie formalism has been applied to infinite

circular cylinders, and which approaches have been taken to solve the resulting equations

numerically. We then proceed to describe the new algorithm that we developed that is

based on the ratios of Bessel functions, and how that algorithm can be implemented.

Finally, we compare the new algorithm with several other published methods.

2. Review of the Mie formalism applied to infinite circular cylinders

We follow the notation introduced in reference [5] and consider an infinite homogeneous

circular cylinder of radius a that is oriented along $\hat{\mathbf{e}}_z$ illuminated by a plane

homogeneous wave of amplitude E_0 propagating in direction $\hat{\mathbf{e}}_i$ in the $\hat{\mathbf{e}}_x$-$\hat{\mathbf{e}}_z$ plane. The

geometry is shown in Figure 1. Let ζ be the angle between the incident wave and the

cylinder axis, and let m be the complex refractive index of the cylinder relative to that of

the surrounding medium that is assumed to be loss-less. If the incident electric field is

parallel to the $\hat{\mathbf{e}}_x$-$\hat{\mathbf{e}}_z$ plane, the scattered electric field can be written as

$$\mathbf{E}_s^{\|} = -\sum_{n=-\infty}^{\infty} E_n \left(b_{nI} \mathbf{N}_n^{(3)} + i a_{nI} \mathbf{M}_n^{(3)} \right), \tag{1}$$

where $E_n = E_0 (-i)^n / k \sin \zeta$, and $\mathbf{N}_n^{(3)}$ and $\mathbf{M}_n^{(3)}$ are the cylindrical vector harmonics

generated by $H_n^{(1)}(kr \sin \zeta) e^{in\phi} e^{-ikz \cos \zeta}$. $H_n^{(1)}$ are the Hankel functions of the first kind,

$k = 2\pi / \lambda$, λ the wavelength of the incident light, r, z, and ϕ the usual cylindrical

coordinates, and a_{nI}, b_{nI}, a_{nII}, and b_{nII} are coefficients defined in Reference [5]. It can

be shown that $a_{-nI} = -a_{nI}$, $b_{-nI} = b_{nI}$, $a_{0I} = 0$, $a_{-nII} = a_{nII}$, $b_{-nII} = -b_{nII}$, $b_{0II} = 0$, and

$a_{-nI} = -b_{nII}$. The scattering and extinction efficiencies defined as the ratios of the cross

sections and the geometrical area ($2aL$ where L is the cylinder length) of the particle are

given by

$$Q_{sca,I} = \frac{2}{x}\left(\left| b_{0I} \right|^2 + 2\sum_{n=1}^{\infty}\left(\left| b_{nI} \right|^2 + \left| a_{nI} \right|^2 \right) \right) \qquad \text{and} \qquad (2)$$

$$Q_{ext,I} = \frac{2}{x}\text{Re}\left\{ b_{0I} 2\sum_{n=1}^{\infty} b_{nI} \right\}, \qquad (3)$$

respectively.

If the incident electric field is perpendicular to the $\hat{\mathbf{e}}_x$-$\hat{\mathbf{e}}_z$ plane, the scattered electric

field can be written as

$$\mathbf{E}_s^{\perp} = -\sum_{n=-\infty}^{\infty} E_n\left(b_{nII}\mathbf{N}_n^{(3)} + ia_{nII}\mathbf{M}_n^{(3)} \right). \qquad (4)$$

The scattering and extinction coefficients in this case are given by

$$Q_{sca,II} = \frac{2}{x}\left(\left| a_{0II} \right|^2 + 2\sum_{n=1}^{\infty}\left(\left| a_{nII} \right|^2 + \left| b_{nII} \right|^2 \right) \right) \qquad \text{and} \qquad (5)$$

$$Q_{ext,II} = \frac{2}{x} \text{Re}\left\{ a_{0II} 2 \sum_{n=1}^{\infty} a_{nII} \right\}, \tag{6}$$

respectively. Within this formalism, the problem of calculating the scattered electric field and the scattering and extinction coefficients is essentially reduced to evaluating the coefficients a_{nI}, b_{nI}, a_{nII}, and b_{nII}.

Convergence of Equations (1) through (6) is obtained as a sum over a finite number of terms n_c. In extensive calculations [13] for spheres it was found that n_c is given by

$$n_c^{(1)} = Round\left(x + 4.05x^{1/3} + 2\right), \tag{7}$$

where the *Round* function indicates the integer closest to the real argument. A similar value has been used for the calculations of cylinders in References [5] and [15]. Barber *et al.* [16] have been found that in certain situations the sums in Equations (1) through (6) only converge if n_c is extended to

$$n_c^{(2)} = Round\left(\max\left(\left(x + 4.05x^{1/3} + 2\right), |mx|\right)\right), \tag{8}$$

for example if internal or scattered field quantities at morphology-dependent resonances of the cylinder are to be calculated.

3. Description of existing algorithms

Calculation of the coefficients a_{nI}, b_{nI}, a_{nII}, and b_{nII} generally requires the calculation of the Bessel functions of the first kind, $J_n(\eta)$ and $J_n(\xi)$, their derivatives with respect to the argument, $J_n'(\eta)$ and $J_n'(\xi)$, as well as the Hankel functions $H_n^{(1)}(\xi)$ and their derivatives with respect to the argument, $H_n^{(1)'}(\xi)$. Here $\xi = x\sin\zeta$,

$\eta = x\sqrt{m^2 - \cos^2\zeta}$, and $x = ka$ is the size parameter.

The evaluation of $J_n(\xi)$ and $H_n^{(1)}(\xi)$ has been considered as numerically not problematic since ξ is real, and standard recurrence method in the direction of decreasing n can be carried out [17]. We have found that this is true for $n \le n_c^{(1)}$, but for $n_c^{(1)} \le n \le n_c^{(2)}$, $J_n(\xi)$ can become very small and the algorithm sometimes become unstable. This is discussed in more detail below. If $J_n(\xi)$ can be evaluated, the calculation of

$H_n^{(1)}(\xi) = J_n(\xi) + iY_n(\xi)$ is less problematic since the evaluation of the Bessel functions of the second kind $Y_n(\xi)$ is numerically stable.

The parameter η, however, can be complex, so that the Bessel functions generally also need to be evaluated for complex arguments. This is difficult when the imaginary part of η is very large, since for a complex number z with $|z| \to \infty$, [17]

$$J_n(z) = \sqrt{2/(\pi z)}\left(\cos(z - n\pi/2 - \pi/4) + e^{|\text{Im}\{z\}|}O\left(|z|^{-1}\right)\right), \qquad (9)$$

and $J_n(z)$ grows exponentially due to the cos term. To address this issue, it has been suggested to reformulate the problem using the logarithmic derivative $D_n(\eta) = J'_n(\eta)/J_n(\eta)$, which is well behaved for large $|\text{Im}\{\eta\}|$. This is similar to calculating the logarithmic derivative $A_n = \psi'_n / \psi_n$ of the Riccati-Bessel functions ψ_n as it has been suggested for scattering from spheres. Du [14] has discussed that the calculation of the logarithmic derivative is generally complicated and even requires a separate treatment for small particles. He and others [18-19] have suggested an alternative, numerically stable approach of reformulating the problem in terms of ratios of the Riccati-Bessel functions, ψ_{n-1}/ψ_n.

4. Formulation of the new algorithm

To address the numerical problems described in the previous Section we apply the approach suggested by Du [14] for spheres to cylinders. We have extended his approach and reformulate the problem in terms of ratios of the Bessel functions defined as

$$r_n(z) = \frac{J_{n-1}(z)}{J_n(z)}, \qquad (10)$$

$$s_n(z) = \frac{Y_{n-1}(z)}{Y_n(z)}, \qquad \text{and} \qquad (11)$$

$$t_n(z) = \frac{Y_n(z)}{J_n(z)}. \qquad (12)$$

Since $r_n(z) = D_n(z) + n/z$, as $D_n(z)$, $r_n(z)$ is well behaved for large arguments. A similar same argument can be made for $s_n(z)$. Since $J_{n-1}(z) + J_{n+1}(z) = 2J_n(z)n/z$ and $Y_{n-1}(z) + Y_{n+1}(z) = 2Y_n(z)n/z$, we can calculate $r_n(z)$ and $s_n(z)$ using the recurrence relations

$$r_n(z) + r_{n+1}^{-1}(z) = \frac{2n}{z} \quad \text{and} \tag{13}$$

$$s_n(z) + s_{n+1}^{-1}(z) = \frac{2n}{z}. \tag{14}$$

In our algorithm $t_n(z)$ needs only be evaluated for real arguments. $t_n(z)$ is well-behaved for $n > |z|$ but can become very large for $n << |z|$. Instead of evaluating $t_n(z)$ directly, we calculate $\ln(|t_n(z)|)$ and the sign of $t_n(z)$ separately using the recurrence relations

$$\ln(|t_n(\eta)|) = \ln(|t_{n-1}(\eta)|) + \ln\left(\left|\frac{r_n(\eta)}{s_n(\eta)}\right|\right) \quad \text{and} \tag{15}$$

$$\text{sgn}(t_n(\eta)) = \text{sgn}(t_{n-1}(\eta))\text{sgn}\left(\frac{r_n(\eta)}{s_n(\eta)}\right), \tag{16}$$

respectively. Here the $\text{sgn}(z)$ is 1 for $z > 0$ and -1 for $z < 0$.

The coefficients for the scattered electric field can then be written as

$$a_{nI} = P_n \frac{C_n V_n - B_n D_n}{W_n V_n + i D_n^2}, \tag{17}$$

$$a_{nII} = -P_n \frac{A_n V_n - i C_n D_n}{W_n V_n + i D_n^2}, \tag{18}$$

$$a_{nII} = -P_n \frac{A_n V_n - i C_n D_n}{W_n V_n + i D_n^2}, \quad \text{and} \tag{19}$$

$$b_{nII} = -i P_n \frac{C_n W_n + A_n D_n}{W_n V_n + i D_n^2}, \tag{20}$$

with

$$A_n = i\xi \left(\xi \left(r_n(\eta) - n/\eta + \frac{\eta n}{\xi^2} \right) - \eta r_n(\xi) \right), \tag{21}$$

$$B_n = \xi \left(m^2 \xi \left(r_n(\eta) - n/\eta + \frac{\eta n}{(m\xi)^2} \right) - \eta r_n(\xi) \right), \tag{22}$$

$$C_n = n\cos(\zeta)\eta\left(\frac{\xi^2}{\eta^2} - 1 \right), \tag{23}$$

$$D_n = C_n, \tag{24}$$

$$V_n = \xi \left(m^2 \xi \left(r_n(\eta) - n/\eta + \frac{\eta n}{(m\xi)^2} \right) - \eta s_n(\xi) \frac{\left(\frac{r_n(\xi)}{s_n(\xi)} + it_n(\xi) \right)}{\left(1 + it_n(\xi) \right)} \right), \tag{25}$$

$$W_n = i\xi \left(\eta s_n(\xi) \frac{\left(\dfrac{r_n(\xi)}{s_n(\xi)} + it_n(\xi) \right)}{\left(1 + it_n(\xi)\right)} - \xi \left(r_n(\eta) - n/\eta + \frac{\eta n}{\xi^2} \right) \right), \quad \text{and} \qquad (26)$$

$$P_n = \frac{1}{\left(1 + it_n(\xi)\right)}. \qquad (27)$$

5. Numerical implementation of the new algorithm

Du [14] derived an estimate of the order of magnitude of the Bessel functions based on the Kapteyn inequality [20]. The number of orders between the moduli of $J_0(z)$ and $J_n(z)$ is approximately

$$l_n(z) = \left(\left| \mathrm{Im}\{z\} \right| - \ln(2) - n \, \mathrm{Re} \left\{ \ln\left(\frac{z}{n} \right) + \sqrt{1 - \left(\frac{z}{n} \right)^2} - \ln\left(1 + \sqrt{1 - \left(\frac{z}{n} \right)^2} \right) \right\} \right) \qquad (28)$$
$$/ \ln(10)$$

If $J_n(z)$ is calculated by upward recurrence, which means that higher orders in n are generated from lower orders, $l_n(z)$ is approximately the number of lost significant digits [14]. The downward recurrence of $J_n(z)$ is numerically stable, and $l_n(z)$ can again be used to estimate the number of significant digits added. The starting point for the downward recurrence n_{mx} is chosen such that $l_{n_{mx}}(z) - l_{n_c}(z)$ is equal or larger than the

desired number of digits in $J_n(z)$. A similar analysis holds for $r_n(z)$, for which we start

the downward recurrence using Equation (13) with $r_{n_{mx}}(z) = (2n_{mx} + 1)/z$ [14].

Since the upward recurrence of $Y_n(z)$ is numerically stable [5], we also calculate $s_n(z)$

by upward recurrence using Equation (14). The algorithm is started by calculating $s_0(z)$

explicitly using the methods described in Reference [5].

Given $r_n(z)$ and $s_n(z)$, $\ln(|t_n(z)|)$ and $\mathrm{sgn}(t_n(z))$ can be calculated using Equations (15)

and (16). Again we start the algorithm by calculating $t_0(z)$ explicitly using the methods

described in Reference [5]. For $|r_n(\xi)/s_n(\xi)| << |t_n(\xi)|$, we approximated Equations (25)

and (26) by

$$V_n \approx \xi\left[m^2\xi\left(r_n(\eta) - n/\eta + \frac{\eta n}{(m\xi)^2} \right) - \eta s_n(\xi) \right] \text{ and} \qquad (29)$$

$$W_n \approx i\xi\left(\eta s_n(\xi) - \xi\left(r_n(\eta) - n/\eta + \frac{\eta n}{\xi^2} \right) \right), \qquad (30)$$

with which all terms in Equations (17) through (20) can be evaluated. For large $|t_n(\xi)|$

the calculation of P_n using Equation (27) can be difficult but that cannot be avoided since

the magnitude of this term is directly related to the magnitude of the inverse of

coefficients a_{nI}, b_{nI}, a_{nII}, and b_{nII}.

6. Comparison with existing algorithms

For the case of normal incidence, Barber and Hill [6] and Bohren and Huffman [5]
published algorithms to calculate the coefficients a_{nI}, b_{nI}, a_{nII}, and b_{nII}. Since our
algorithm includes the special case of illumination at normal incidence when we set
$\zeta = 90^o$, we can compare the results of these algorithms directly to ours. Mackowski
[15] implemented the algorithm described in reference [5] for illumination at oblique
incidence but did not carry out extensive numerical optimizations. In the following we
also compare the results from this algorithm to ours to assure that it gives correct results
for $\zeta \neq 90^o$.

We found it convenient to compare the scattering efficiency $Q_{sca,I}$ as a function of the
size parameter x. Figures 2 (a) through (d) show $Q_{sca,I}$ for a size parameter ranging
from 10 to 11, calculated using the different algorithms. We assumed illumination at
normal incidence ($\zeta = 90^o$) and $m = 1.5$. Equation (2) was evaluated using terms up to
$n_c = n_c^{(1)}$. We found that our algorithm agrees very well with the other published
algorithms. As shown in Figure 3, including higher order terms in the calculations for
example by using $n_c = n_c^{(2)}$ does not alter the results significantly in this case.

We now consider a larger size parameter x ranging from 1000 to 1001. Figure 4 (a)
shows $Q_{sca,I}$ as a function of the size parameter x calculated using the algorithm

described in this paper with $n_c = n_c^{(2)}$. Figure 4 (b) shows $Q_{sca,I}$ calculated using the algorithm described by Bohren and Huffman [5] with summation cutoffs $n_c^{(1)}$, $n_c^{(2)}$, and

$$n_c^{(3)} = Round\left(\max\left(\left(x + 4.05x^{1/3} + 2\right), |mx|, |m|\left(x + 4.05x^{1/3} + 2\right)\right)\right).$$ (31)

We found that for the Bohren and Huffman algorithm, $n_c^{(3)}$ summation terms in Equation (2) are necessary to reach true convergence, which is primarily due to the lack of convergence of the logarithmic derivative $D_n(\eta)$. In Table I we compare the calculated value of $D_0(1500)$ with the calculated values for different summation cutoffs n_c. The algorithm by Bohren and Huffman [5] only converges for $n_c = n_c^{(3)}$. The code we propose converges already with $n_c = n_c^{(2)}$.

If we consider even larger cylinders with a size parameter x ranging from 5000 to 5001, the value of our approach of using the ratios of Bessel functions becomes even clearer. Figure 5 (a) shows $Q_{sca,I}$ as a function of the size parameter x calculated using the algorithm described in this paper with $n_c = n_c^{(2)}$. Figure 5 (b) shows $Q_{sca,I}$ calculated using the algorithm described by Bohren and Huffman algorithm [5] with $n_c = n_c^{(1)}$, which is not sufficient to achieve convergence. We found that the latter algorithm is not able to calculate the Bessel functions of the first kind for $n_c = n_c^{(2)}$ or $n_c = n_c^{(3)}$ since the numbers that are encountered are too small to be represented by double-precision complex values.

To verify that the algorithm described in this paper also delivers correct results for illumination at oblique incidence ($\zeta \neq 90^o$), we calculated $Q_{sca,I}$ as a function of the size parameter x for $\zeta = 30^o$, and compared this with values obtained from the algorithm from Reference [15]. As can be seen in Figure 6, we obtained very good agreement. Numerical instabilities limits the algorithm from Reference [15] to relatively small size parameters, whereas for our algorithm these restrictions are much more relaxed.

7. Summary and Conclusions

A Mie-type analysis of the problem of the scattering of a plane-wave from an infinite homogeneous circular cylinder requires the calculation of the coefficients a_{nI}, b_{nI}, a_{nII}, and b_{nII}. In this paper we have presented a new algorithm to calculate these parameters based on the calculation of the ratios of Bessel functions instead of calculating the Bessel functions or their logarithmic derivatives directly. We have found that this algorithm agrees with existing algorithms for light illuminating the cylinder at normal and oblique incidence, given that the existing algorithms converge. We have further shown that our algorithm also converges in cases of very large cylinder diameter to wavelength ratios, for which other algorithms sometimes do not.

References

[1] R.K. Mueller, M. Kaveh, and G. Wade, "Reconstructive tomography and applications to ultrasonics", Proc. IEEE **67**, 567-587 (1979).

[2] R.K. Mueller, M. Kaveh, R.D. Iverson, in: A.F. Metherell (Ed.), Acoustical Imaging **8**, p. 615, Plenum Press, New York (1980).

[3] E. Wolf, "Three-dimensional structure determination of semi-transparent objects from holographic data", Opt. Commun. **1**, 153-156 (1969).

[4] O.R. Halse, K.K. Stamnes, and A.J. Devaney, "Three-dimensional diffraction tomography by two-dimensional sectioning", Opt. Commun. **224**, 185-195 (2003).

[5] C.F. Bohren and D.R. Huffman, "Absorption and Scattering of Light by Small Particles", Wiley-Interscience, New York, 1983.

[6] P.W. Barber and S.C. Hill, "Light Scattering by Particles: Computational Methods", World Scientific, River Edge, New Jersey, 1990.

[7] H.C. van de Hulst, "Light Scattering by Small Particles", Dover, New York, 1981.

[8] M. Kerker, "The Scattering of Light and Other Electromagnetic Radiation", Academic Press, New York (1969).

[9] M. Kerker, D. Cooke, W.A. Farone, and R.T. Jacobson, "Electromagnetic scattering from an infinite circular cylinder at oblique incidence: I. Radiance functions for m=1.46", J. Opt. Soc. Am. **56**, 487-491 (1966).

[10] L. Infeld, "The influence of the width of the gap upon the theory of antennas", Q. Appl. Math. **5**, 113-132 (1947).

[11] J.V. Dave, "Scattering of electromagnetic radiation by a large, absorbing sphere", IBM J. Res. Dev. **13**, 302-313 (1969).

[12] W.J. Lentz, "Generating Bessel functions in Mie scattering calculations using continued fractions", Appl. Opt. **15**, 668-671 (1976).

[13] W.J. Wiscombe, "Improved Mie scattering algorithms", Appl. Opt. **19**, 1505-1509 (1980).

[14] H. Du, "Mie-scattering calculation", Appl. Opt. **43**, 1951-1956 (2004).

[15] D. Mackowski, private communication.

[16] P.W. Barber, J.F. Owen, and R.K. Chang, "Resonant scattering for characterization of axisymmetric dielectric objects", IEEE Trans. Antennas Propag. **AP-30**, 168-172 (1982).

[17] M. Abramowitz and I.A. Stegun, "Handbook of Mathematical Functions with Formulas, Graphs, and Mathematical Tables", Dover, New York, 1965.

[18] R.T. Wang and H.C. van de Hulst, "Rainbows: Mie computations and the Airy approximation", Appl. Opt. **30**, 106-117 (1991).

[19] V.E. Cachorro and L.L. Salcedo, "New improvements for Mie scattering calculations", J. Electromagn. Waves. Appl. **5**, 913-926 (1991).

[20] G.N. Watson, "A Treatise on the Theory of Bessel Functions", Cambridge University Press, London, 1966.

Table Captions

Table I: The logarithmic derivative $D_0(1500)$ calculated by the algorithm described by Bohren and Huffman [5] and the actual value for different summation cutoffs n_c.

Tables

	$n_c = n_c^{(1)} = 1041$	$n_c = n_c^{(2)} = 1500$	$n_c = n_c^{(3)} = 1562$	actual value
$D_0(1500)$	-0.8794	-0.8794	-0.8005	-0.8005

Table I

Figure Captions

Figure 1: Geometry of an inifinite cylinder at oblique illumination by a plane wave.

Figure 2: Scattering efficiency $Q_{sca,I}$ for incident light with the electric field is parallel to the $\hat{\mathbf{e}}_x$-$\hat{\mathbf{e}}_z$ plane as a function of size parameter calculated using the algorithms (a) described in this paper, (b) by Bohren and Huffman, (c) by Mackowski, and (d) by Barber and Hill. The calculations used 1000 points.

Figure 3: Comparison of $n_c = n_c^{(1)}$ and $n_c = n_c^{(2)}$. Scattering efficiency $Q_{sca,I}$ as a function of size parameter using the algorithm described in this paper. The calculations used 1000 points.

Figure 4: Scattering efficiency $Q_{sca,I}$ as a function of size parameter calculated using the algorithms (a) described in this paper and (b) by Bohren and Huffman. The calculations used 10000 points. For the results shown in (b) we used different summation cutoffs n_c. The curves for $n_c = n_c^{(1)}$ and $n_c = n_c^{(2)}$ are identical. The peaks are due to morphology-dependent resonances of the cylinder.

Figure 5: Scattering efficiency $Q_{sca,I}$ as a function of size parameter calculated using the algorithms (i) described in this paper with $n_c = n_c^{(2)}$ and (ii) by Bohren and Huffman with $n_c = n_c^{(1)}$. The calculations used 10000 points.

Figure 6: Scattering efficiency $Q_{sca,I}$ as a function of size parameter calculated using the algorithms (a) described in this paper and (b) from Reference [Mack] for an incident angle of $\zeta = 30^o$.
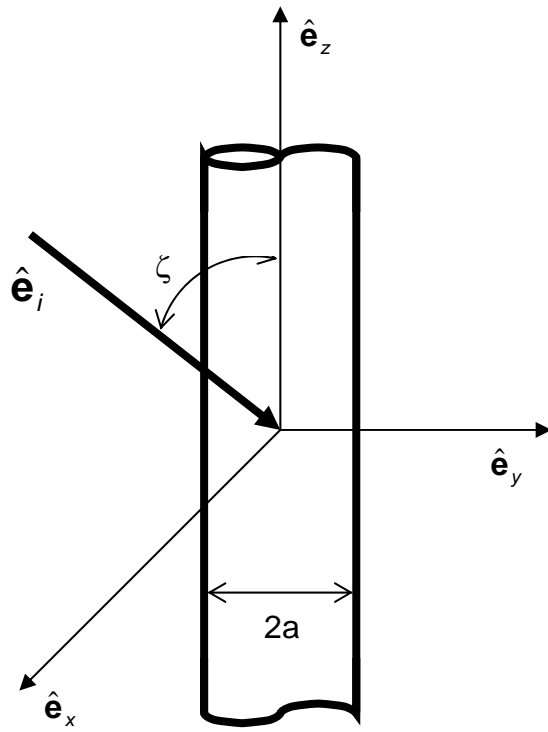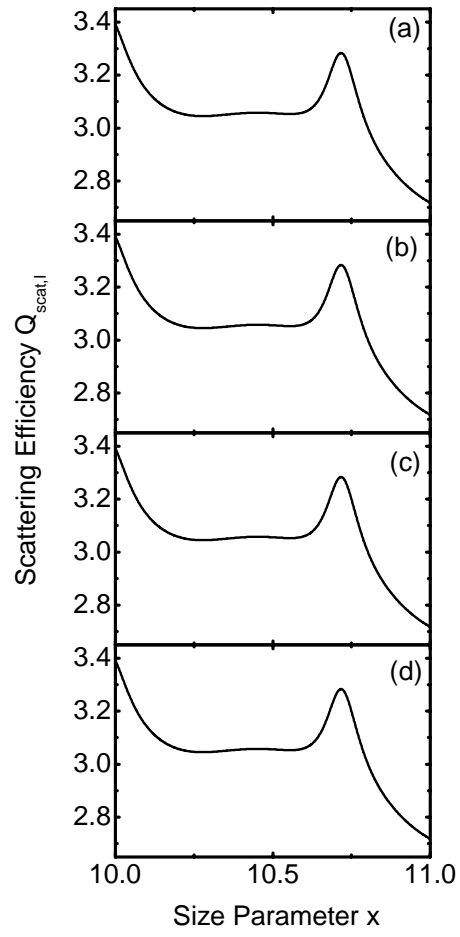
Figure 1 (Hau-Riege)

Figure 2 (Hau-Riege)
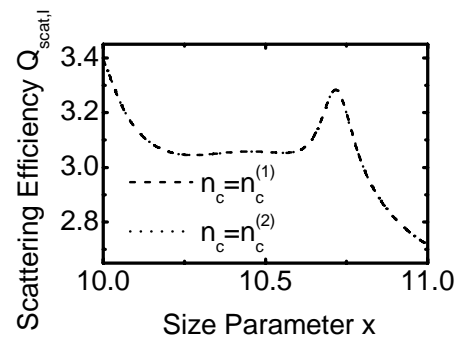
Figure 3 (Hau-Riege)
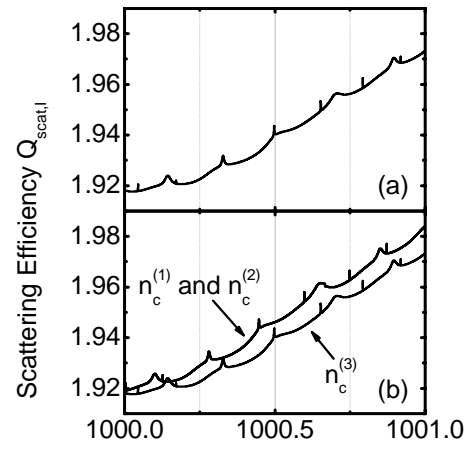
Figure 4 (Hau-Riege)
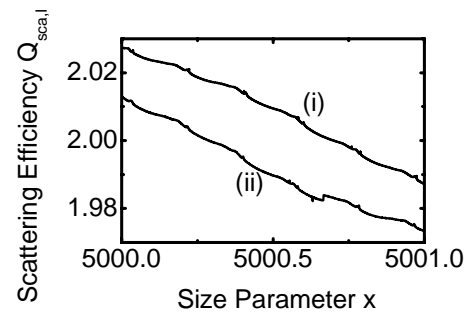
Figure 5 (Hau-Riege)

Figure 6 (Hau-Riege)